FULL PAPER

Dalton
www.rsc.org/dalton

A new NS_4 quinquedentate macrocyclic ligand: synthesis, structure and properties of its Ni(II), Pd(II), Pt(II), Cu(II), Cu(I) and Ag(I) complexes †

Muthalagu Vetrichelvan, Yee-Hing Lai * and Kum Fun Mok
Department of Chemistry, National University of Singapore, 3 Science Drive 3, Singapore 117543. E-mail: chmlaiyh@nus.edu.sg

Received 26th June 2002, Accepted 21st November 2002
First published as an Advance Article on the web 23rd December 2002

An aza-thia macrocycle 2,5,14,17-tetrathia[6](1,2)benzeno[6](2,6)pyridinophane (**11**) and its complexes with Ni(II), Pd(II), Pt(II), Cu(II), Cu(I) and Ag(I) were synthesized and their crystal structures were determined. Ni(II) forms an octahedral complex coordinated to NS_3 of the ligand and two chlorine atoms of the metal salt; one of the sulfurs in the ligand is uncoordinated. The crystal structures of $[Pd\cdot\mathbf{11}][PF_6]_2$ and $[Pt\cdot\mathbf{11}][PF_6]_2$ confirm a $[NS_3 + S]$ coordination in both complexes. NMR spectroscopic studies indicate that only one form of each complex is present in solution. Cu(II), Cu(I) and Ag(I) complexes of the macrocycle adopt a geometry in between a square pyramid and a trigonal bipyramid with NS_4 coordination around the metal ions in $[Cu\cdot\mathbf{11}][ClO_4]_2$, $[Cu\cdot\mathbf{11}][PF_6]$ and $[Ag\cdot\mathbf{11}][PF_6]$. The electronic and redox properties of $[Pd\cdot\mathbf{11}][PF_6]_2$, $[Pt\cdot\mathbf{11}][PF_6]_2$ and the copper complexes in acetonitrile have been examined. The complexation behaviour of the macrocycle, **11**, has also been studied in solution and found to lack good selectivity towards the selected transition metal ions.

Introduction

The coordination chemistry of polyaza, polythia and mixed aza-thia macrocyclic ligands has attracted much attention in recent times. These macrocycles show the remarkable ability to form stable and inert complexes with a wide range of d- and p-block metals, in many cases forcing the metal centre to adopt unusual coordination geometries or oxidation states.[1–10] The presence of sulfur donors as part of a macrocyclic ligand has been shown to stabilize low valent metal complexes as well as to have a marked influence on the coordination geometry at the metal centre. Our interest in coordination chemistry focuses on the study of macrocyclic ligands with mixed heteroatoms since these are expected to exhibit novel metal coordination properties. Examples of quinquedentate macrocycilc ligands containing N and S are few although the coordination chemistry of macrocyclic ligands such as **1**–**6** has been reported.[11–15]

To the best of our knowledge, the title compound **11** in this work is the first example of a NS_4 pyridine-containing quinquedentate macrocycle. We report herein the synthesis of the [17]aneNS_4 macrocycle, **11**, its complexation behaviour with platinum and the coinage group metals, and a UV-visible absorption study. The redox properties of the palladium, platinum and copper complexes, and the extraction properties of the ligand **11** were also studied. The platinum and coinage group metals were selected because of the ability of soft thioether ligands to bind very effectively to soft metal ions. The interest in this type of ligands is indicated by studies on the coordination chemistry of the mixed donor macrocycles [18]aneN_2S_4 and Me_2[18]aneN_2S_4 summarized by Reid and Schröder.[16]

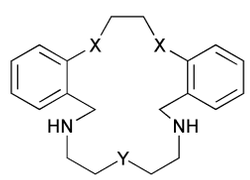

1, X = S; Y = S
2, X = S, Y = NH

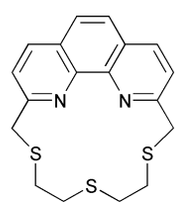

3

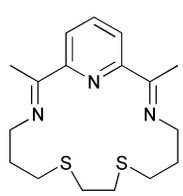

4

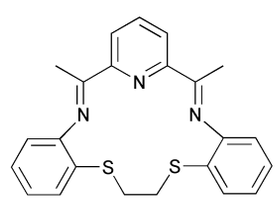

5

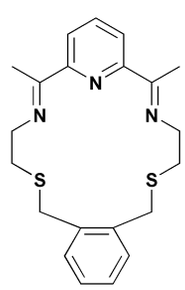

6

Experimental

CAUTION! Perchlorate salts are potentially explosive and should be handled with care.

Materials and physical measurements

^{1}H and ^{13}C NMR spectra were recorded on a Bruker ACF 300 Fourier-transform spectrometer. All chemical shifts are reported in ppm downfield from the tetramethylsilane internal standard. Mass spectra were recorded on a VG Micromass 7035 spectrometer at 70 eV, electron impact being used. Elemental analyses were performed by the Chemical and Molecular Analysis Centre, Department of Chemistry, National University of Singapore. The electronic spectra were recorded using a HP 8452A diode-array UV/Vis spectrophotometer. Cyclic voltammograms were recorded using a single compartment three-

† Presented at ISMC-2001 held in Fukuoka, Japan from July 15–20, 2001.

Electronic supplementary information (ESI) available: synthetic scheme for macrocyclic complexes **12**–**17**; views of **12**, **15** and **16**; cyclic voltammograms of **13** and **14**. See http://www.rsc.org/suppdata/dt/b2/b206182a/

DOI: 10.1039/b206182a

electrode cell. A platinum disc of 3 mm in diameter was used as a working electrode. The counter electrode consisted of a platinum wire. All the potentials were measured against the Ag–AgCl couple. An EG&G Princeton Applied Research 273 potentiostat, controlled by M270 software, was used to measure all the electrochemical data. Acetonitrile used for electrochemical studies was triply distilled under nitrogen from calcium hydride and stored over 4 Å molecular sieves. TEAFB employed as a supporting electrolyte was vacuum dried for 24 h prior to use. All solutions were purged with dry argon for 15 min prior to any electrochemical study. The following compounds were prepared according to the literature: *o*-xylenebis(1-hydroxy-3-thiapropane),[17] *o*-xylenebis(1-chloro-3-thiapropane)[17] and 2,6-bis(mercaptomethyl)pyridine.[18] All solvents used in the reactions were dried by conventional methods.

Synthesis

Macrocycle 11. A solution of *o*-xylenebis(1-chloro-3-thiapropane) (1.77 g, 6.0 mmol) and 2,6-bis(mercaptomethyl)pyridine (1.03 g, 6.0 mmol) in DMF (100 mL) was added slowly over a period of 8–10 h to a well stirred suspension of Cs_2CO_3 (3.91 g, 12.0 mmol) in DMF (700 mL) maintained at 55–65 °C under an atmosphere of N_2. The reaction temperature was maintained at 55–65 °C for another 12 h. After addition the mixture was cooled to room temperature and stirred for a further 12 h. The DMF was removed under vacuum and the resulting residue was extracted with dichloromethane, washed with aq. NaOH followed by water. The organic layers were combined, dried and concentrated under reduced pressure. The resulting residue was chromatographed on silica gel using a mixture of hexane–ethyl acetate (4 : 1) to give the macrocycle **11** as colourless crystals. Yield 51%; mp 102–104 °C. Analytical data: Found: C, 57.4; H, 5.8; N, 3.7; S, 31.4. Calc. for $C_{19}H_{23}NS_4$: C, 57.9; H, 5.8; N, 3.8; S, 32.5%. MS: *m*/*z* 393.6 (M^+). ^{1}H NMR ($CDCl_3$): δ 7.65 (t, 1H), 7.35–7.20 (m, 6H), 3.88 (s, 4H), 3.82 (s, 4H), 2.8–2.7 (m, 8H). ^{13}C NMR ($CDCl_3$): δ 158.5, 137.7, 135.9, 130.3, 127.6, 121.25, 37.9, 33.6, 32.2, 31.6.

Complex 12. A solution of **11** (102 mg, 0.26 mmol) in dichloromethane (10 mL) was added to a solution of $NiCl_2 \cdot 6H_2O$ (62 mg, 0.26 mmol) in methanol (10 mL). The mixture was stirred for 1 h and diffusion of ether into the resultant mixture gave green crystals of **12**. The crystals were insoluble in common organic solvents except DMSO. Yield: 68%; mp 195–197 °C (dec.). Analytical data: Found: C, 42.0; H, 4.3; N, 2.67; S, 21.7. Calc. for $C_{19}H_{23}Cl_2NNiS_4$: C, 43.6; H, 3.8; N, 2.67; S, 24.5%. FAB MS *m*/*z*: 487.0 [Ni·**11**·Cl], 452.0 [Ni·**11**]. UV-Vis (DMSO): λ_{max}/nm (ε_{max}/dm^3 mol^{-1} cm^{-1}): 240 (20656), 279 (21379), 308 (11598), 586 (41), 664 (39).

Complex 13. A solution of **11** (102 mg, 0.26 mmol) in dichloromethane (10 mL) was added to $PdCl_2(CH_3CN)_2$ (68 mg, 0.26 mmol) in methanol (10 mL) and the mixture was stirred at room temperature for 10 h. Addition of a large excess of NH_4PF_6 and concentration of the solution *in vacuo* afforded red–orange complex **13**. Yield: 72%; mp 176 °C (dec.). Analytical data: Found: C, 28.5; H, 2.4; N, 2.0; S, 15.5. Calc. for $C_{19}H_{23}NS_4PdP_2F_{12} \cdot H_2O$: C, 28.3; H, 2.8; N, 1.8; S, 15.8%. FAB MS: *m*/*z* 644.4 [Pd·**11**·PF_6], 499.5 [Pd·**11**]. ^{1}H NMR (CD_3CN): δ 8.25 (t, 1H), 8.0–7.5 (m, 6H), 3.50–5.80 (m, 16H). ^{13}C NMR (CD_3COCD_3): δ 162.5, 161.5, 142.4, 132.1, 130.1, 129.3, 47.3, 46.1, 39.9, 38.2. UV-Vis (MeCN): λ_{max}/nm (ε_{max}/dm^3 mol^{-1} cm^{-1}) 240 (28320), 290 (30570) and 490 (154).

Complex 14. This complex was isolated as yellow crystals by a similar procedure to that described for **13**. Yield: 78%; mp 197–198 °C (dec.). Analytical data: Found: C, 25.2; H, 2.5; N, 1.9; S, 14.1. Calc. for $C_{19}H_{23}NS_4PtP_2F_{12} \cdot H_2O$: C, 25.4; H, 2.5; N, 1.6; S, 14.3%. FAB MS: *m*/*z* 733.5 [Pt·**11**·PF_6], 588.5 [Pt·**11**]. ^{1}H NMR (CD_3CN): δ 8.40 (t, 1H), 8.0–7.4 (m, 6H), 3.40–5.20 (m, 16H). ^{13}C NMR (CD_3COCD_3): δ 164.2, 163.5, 144.2, 139.48, 133.54, 132.75, 47.7, 43.0, 41.0, 38.7. UV-Vis (MeCN): λ_{max}/nm (ε_{max}/dm^3 mol^{-1} cm^{-1}): 230 (23520), 264 (21269).

Complex 15. A solution of **11** (40 mg, 0.1 mmol) in dichloromethane (10 mL) was added to a solution of $Cu(ClO_4)_2 \cdot 6H_2O$ (38 mg, 0.1 mmol) in methanol (10 mL). A dark green crystalline complex of **15** was formed after stirring the mixture for 10–15 min. Yield: 85%. Analytical data: Found: C, 33.8; H, 3.7; N, 2.2; S, 19.1. Calc. for $C_{19}H_{25}Cl_2CuNO_9S_4$: C, 33.8; H, 3.7; N, 2.1; S, 19.0%. FAB MS: *m*/*z* 456.0 [Cu·**11**]. UV-Vis (MeCN): λ_{max}/nm (ε_{max}/dm^3 mol^{-1}cm^{-1}) 430 (3950), 598 (550).

Complex 16. A solution of $AgNO_3$ (9 mg, 0.05 mmol) and a large excess of NH_4PF_6 in methanol (8 mL) was diffused into a solution of **11** (20 mg, 0.05 mmol) in dichloromethane (4 mL). After 1 h, colourless crystals of complex **16** were formed that were relatively light sensitive. The crystals were insoluble in common organic solvents. Yield: 78%; mp 204 °C (dec.). Analytical data: Found: C, 34.8; H, 3.6; N, 2.6; S, 20.1. Calc. for $C_{19}H_{23}AgNPF_6S_4$: C, 35.3; H, 3.6; N, 2.2; S, 19.9%. FAB MS: *m*/*z* 501.6 [Ag·**11** + H].

Complex 17. A solution of **11** (44 mg, 0.112 mmol) in dichloromethane (10 mL) was added to a solution of $CuCl_2 \cdot 2H_2O$ (15 mg, 0.112 mmol) in methanol (10 mL). The precipitates formed after stirring the solution for 3–4 h were removed by filtration. The addition of a large excess of NH_4PF_6 to the filtrate followed by slow evaporation of the solvents gave a yellow–green precipitate of complex **17**. Yield: 58%; mp 158–160 °C (dec.). Analytical data: Found: C, 36.2; H, 3.7; N, 2.6; S, 28.0. Calc. for $C_{19}H_{23}NCuPF_6S_4$: C, 37.9; H, 3.2; N, 2.4; S, 21.3%. FAB MS: *m*/*z* 457.9 [Cu·**11**]. ^{1}H NMR (CD_3CN): δ 7.80 (t, 1H), 7.3–7.6 (m, 6H), 4.00 (s, 4H), 4.20 (s, 4H), 3.14 (t, 4H), 2.92 (t, 4H). ^{13}C NMR (CD_3CN): δ 162.5, 142.7, 141.1, 137.4, 134.1, 128.8, 42.1, 41.5, 38.3, 36.7. UV-Vis (MeCN): λ_{max}/nm (ε_{max}/dm^3 mol^{-1} cm^{-1}): 426 (2334), 596 (304).

Crystallographic data collection and refinement

Details of the crystal data and refinement of the structures are summarised in Table 1. All compounds were analysed at the Chemical and Molecular Analysis Centre, Department of Chemistry, National University of Singapore. Data collection was carried out at 293 K using graphite monochromated Mo-Kα radiation (λ = 0.71073 Å) on a Siemens CCD diffractometer. Structures were solved by the Patterson (**14** and **17**) or direct (**11**, **12**, **13**, **15** and **16**) methods. All non-hydrogen atoms were refined anisotropically, except for those of solvent molecules where present. Refinement was by full-matrix least-squares based on F^2 using SHELXL 93.[19] Hydrogen atoms were introduced at a fixed distance from carbon atoms and their isotropic thermal parameters were on the riding mode of the parent atoms.

CCDC reference numbers 188671–188677.

See http://www.rsc.org/suppdata/dt/b2/b206182a/ for crystallographic data in CIF or other electronic format.

Results and discussion

Syntheses

A common approach to the synthesis of sulfur-containing macrocyclic ligands invokes carbon–sulfur bond formation in a bimolecular cyclization reaction. Thus the ligand **11** was synthesised by a coupling reaction (Scheme 1) between *o*-xylene-

Table 1 Crystallographic data for compounds **11**–**17**

	11	**12**	**13**	**14**	**15**	**16**	**17**
Chemical formula	$C_{19}H_{23}NS_4$	$C_{19}H_{23}Cl_2NNiS_4$	$C_{19}H_{25}F_{12}NOP_2PdS_4$	$C_{19}H_{25}F_{12}NOP_2PtS_4$	$C_{19}H_{25}Cl_2CuNO_9S_4$	$C_{19}H_{23}AgF_6NPS_4$	$C_{19}H_{23}CuPF_6NS_4$
Formula weight	393.62	523.23	807.98	896.67	674.08	646.46	602.13
T/K	293(2)	293(2)	293(2)	293(2)	293(2)	293(2)	293(2)
λ/Å	0.71073	0.71073	0.71073	0.71073	0.71073	0.71073	0.71073
Crystal system	Monoclinic	Monoclinic	Monoclinic	Monoclinic	Triclinic	Triclinic	Triclinic
Space group	$P2(1)/c$	$P2(1)/n$	$P2(1)/n$	$P2(1)/n$	$P\bar{1}$	$P\bar{1}$	$P\bar{1}$
a/Å	18.2741(7)	7.8184(1)	8.0993(1)	8.0437(1)	11.1837(1)	9.2538(3)	9.2285(2)
b/Å	4.7815(2)	24.2113(1)	20.1018(1)	20.2495(2)	11.5515(1)	12.0217(4)	11.6204(2)
c/Å	22.8791(9)	11.6019(2)	17.3608(3)	17.4965(3)	12.7592(1)	12.5274(4)	13.0124(3)
α/°	90.0	90.0	90.0	90.0	100.950(1)	106.837(1)	105.621(1)
β/°	97.884(1)	102.306(1)	91.526(1)	91.375(1)	115.962(1)	108.836(1)	101.527(1)
γ/°	90.0	90.0	90.0	90.0	100.950(1)	102.033(1)	113.172(1)
V/Å^3	1980.22(14)	2145.71(5)	2825.52(6)	2849.03(7)	1321.17(2)	1190.23(7)	1159.45(4)
Z	4	4	4	4	2	2	2
μ/mm^{-1}	0.481	1.548	1.163	5.427	1.394	1.321	1.428
F(000)	832	1080	1608	1736	690	648	612
Crystal size/mm^3	0.40 × 0.18 × 0.10	0.25 × 0.22 × 0.2	0.18 × 0.16 × 0.08	0.45 × 0.10 × 0.10	0.40 × 0.40 × 0.30	0.32 × 0.20 × 0.08	0.20 × 0.12 × 0.10
Reflections collected	10990	13063	15952	16298	10763	9822	9662
Independent reflections	4322 R(int) = 0.0323	4722 R(int) = 0.0263	5721 R(int) = 0.0443	5785 R(int) = 0.0297	5280 R(int) = 0.0158	4804 R(int) = 0.0244	4705 R(int) = 0.0284
Data/restraints/parameters	4320/0/217	4721/0/244	5721/0/356	5785/0/356	5280/0/325	4803/0/289	4705/0/289
Final R indices [$I > 2\sigma(I)$]	$R1$ = 0.0490, $wR2$ = 0.1012	$R1$ = 0.0382, $wR2$ = 0.0757	$R1$ = 0.0578, $wR2$ = 0.1305	$R1$ = 0.0345, $wR2$ = 0.0817	$R1$ = 0.0413, $wR2$ = 0.1183	$R1$ = 0.0363, $wR2$ = 0.0863	$R1$ = 0.0536, $wR2$ = 0.1286
R indices (all data)	$R1$ = 0.0844, $wR2$ = 0.1331	$R1$ = 0.0548, $wR2$ = 0.0831	$R1$ = 0.0966, $wR2$ = 0.1517	$R1$ = 0.0501, $wR2$ = 0.0893	$R1$ = 0.0482, $wR2$ = 0.1233	$R1$ = 0.0532, $wR2$ = 0.1037	$R1$ = 0.0827, $wR2$ = 0.1448

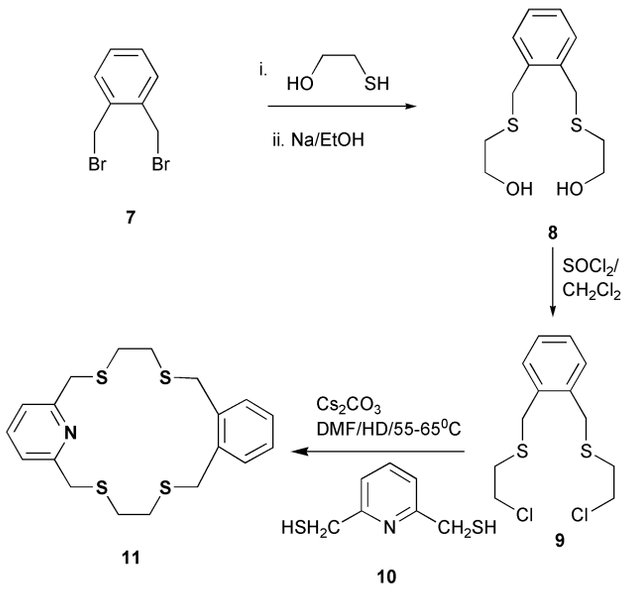

Scheme 1 Synthetic scheme for the preparation of the macrocycle **11**.

bis(1-chloro-3-thiapropane)[17] **9** and 2,6-pyridinedimethanethiol[18] **10** in a yield of about 50%. This macrocycle is soluble in a number of organic solvents such as CH_2Cl_2, $CHCl_3$ and CH_3CN, and could also be readily recrystallised from methanol or acetone. The ^1H NMR spectrum of the ligand shows three distinct sets of resonances: multiplets for the aromatic protons at 7.65–7.20 ppm, a pair of singlets for the benzylic protons at 3.88 and 3.82 ppm, respectively, and a multiplet at 2.82–2.70 ppm corresponding to overlapping methylene proton signals. Colourless crystals of the macrocycle **11** were obtained by slow evaporation of a solution of **11** in a mixture of CH_2Cl_2 and methanol.

The metal complexes **11**–**15** of the macrocycle **11** were prepared by mixing the appropriate metal salts and the ligand, and the details are given in the Experimental section. The reaction of copper(II) chloride dihydrate with one molar equivalent of the ligand **11** followed by addition of an excess of NH_4PF_6 gave unexpectedly a copper(I) complex **16**. The stoichiometric formula of [Cu·**11**][PF_6] was fully supported by its mass spectrum and the results from an elemental analysis both of which indicated the presence of only one PF_6^- counter anion. This was further confirmed by an X-ray crystallographic analysis with the coordination environment and bond distances to Cu inconsistent with a copper(II) complex. However, the pale colour of the solid complex isolated from the reaction might indicate the presence of the copper(II) complex as a minor product.

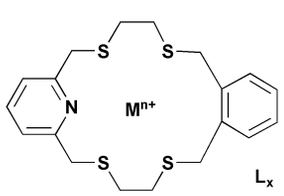

Complex	M^{n+}	L	x
12	Ni(II)	Cl	2
13	Pd(II)	PF_6	2
14	Pt(II)	PF_6	2
15	Cu(II)	ClO_4	2
16	Ag(I)	PF_6	1
17	Cu(I)	PF_6	1

The reduction of Cu(II) ion without a reducing agent is an interesting phenomenon in relation to the action of ligands having sterically hindered conformations. This type of auto-reduction may happen either due to the electronic properties of the donors of the ligand or the geometry of the complexes formed. In this case we believe that the geometry of the metal complexes may have played a vital role. If the sulfur atoms in **11** are replaced by oxygen such auto-reduction does not occur, which further supports the above explanation. Hence, if the geometry of a complex could be controlled to result in a preference for Cu(I) over Cu(II), the reduction of copper(II) complexes and thus synthesis of copper(I) complexes may be made possible. The auto-reduction of copper(II) to copper(I) in this system is however not fully understood.

Structure description of 11

The crystal structure of **11** (Fig. 1) shows that the macrocycle is non-planar and the two aromatic rings lie at an angle of 36.1°. The torsion angles of S–CH_2–CH_2–S (174.8 and 180.0°) demonstrate the propensity for this linkage to adopt an *anti* conformation and that all four sulfur atoms are in exodentate positions. The presence of *o*-xylyl and pyridine rings did not result in any endodentate sulfur atoms with the increase in ring rigidity. However, it may cause, among the four C–C–S–C linkages, two of them to adopt the *gauche* conformation and the other pair show an *anti* conformation. Selected bond distances and angles are summarized in Table 2.

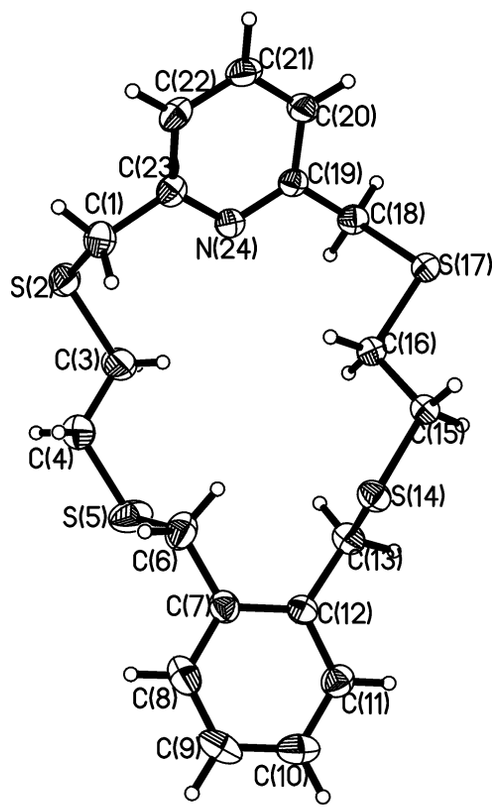

Fig. 1 ORTEP[39] drawing of the macrocycle **11**.

Structure description of complex 12

Green crystals of **12** suitable for X-ray diffraction study were obtained by a slow diffusion of diethyl ether into a solution of the complex in CH_2Cl_2–MeOH mixture. The crystal structure of **12** (Fig. 2) shows that the complex is six-coordinated with a distorted octahedral geometry. A square plane made up of three benzylic thio-ethers and one chlorine atom of the metal salt coordinated to the nickel [Ni–S(2) 2.380(1), Ni–S(5) 2.524(1), Ni–S(17) 2.405(1) and Ni–Cl(1) 2.375(1) Å] with pyridine N(24) and Cl(2) occupying the axial positions of the octahedron. Deviation from the square plane is only about 0.02 Å. The Ni–N(24) bond distance in the nickel complex falls within the range of 2.03–2.16 Å observed previously for coordinate bonds from neutral nitrogen atoms in high spin nickel(II) complexes of macrocyclic ligands.[20] The mean Ni–S and Ni–Cl bond distances are also within the ranges observed for octahedral nickel(II) complexes.[21–26] Angles around the nickel centre are close to 90° [N(24)–Ni–Cl(1) 88.55(6), N(24)–

Table 2 Selected bond distances (Å) and angles (°) with e.s.d.s in parentheses for the ligand **11** and the complexes **12**–**17**

Macrocycle **11**					
C(1)–S(2)	1.803(3)	S(5)–C(6)	1.800(3)	S(2)–C (3)	1.810(3)
C(12)–C(13)	1.504(4)	C(3)–C(4)	1.449(5)	C(13)–S(14)	1.822(3)
C(4)–S(5)	1.808(3)	S(17)–C(18)	1.815(3)	C(6)–C(7)	1.515(4)
C(1)–S(2)–C(3)	102.4(2)	C(5)–C(6)–C(7)	110.2(2)	C(1)–C(23)–N(24)	117.3(2)
C(6)–C(7)–C(8)	118.9(3)	C(3)–C(4)–C(5)	115.6(3)	C(6)–C(7)–C(12)	122.2(3)
C(4)–C(5)–C(6)	102.1(2)	C(19)–N(24)–C(23)	118.1(2)	C(4)–C(3)–S(2)	114.3(3)
S(2)–C(1)–C(23)	115.2(2)				
Complex **12**					
Ni–S(2)	2.380(1)	Ni–N(24)	2.084(2)	Ni–S(5)	2.524(1)
Ni–Cl(1)	2.375(1)	Ni–S(17)	2.405(1)	Ni–Cl(2)	2.362(1)
N(24)–Ni–Cl(1)	88.55(6)	S(5)–Ni–Cl(1)	169.21(3)	N(24)–Ni–Cl(2)	176.10(6)
S(5)–Ni–Cl(2)	95.41(3)	S(2)–Ni–N(24)	84.52(7)	S(17)–Ni–Cl(1)	92.24(3)
S(2)–Ni–S(17)	167.61(3)	Cl(1)–Ni–Cl(2)	95.35(3)	S(5)–Ni–N(24)	81.47(6)

Complexes **13** and **14**	**13**, M = Pd(II)	**14**, M = Pt(II)
M–N(24)	2.024(6)	2.026(5)
M–S(2)	2.260(2)	2.262(2)
M–S(5)	2.312(2)	2.2980(1)
M–S(17)	2.326(2)	2.3074(1)
N(24)–M–S(2)	84.02(2)	84.0(2)
N(24)–M–S(5)	171.8(2)	171.0(2)
N(24)–M–S(17)	85.02(2)	85.31(2)
S(2)–M–S(5)	89.54(8)	89.59(7)
S(2)–M–S(17)	162.23(7)	163.45(6)
S(5)–M–S(17)	102.49(7)	102.24(6)

Complexes **15**–**17**	**15**, M = Cu(II)	**16**, M = Ag(I)	**17**, M = Cu(I)
M–N(24)	2.005(1)	2.378(3)	2.103(3)
M–S(2)	2.314(1)	2.648(1)	2.554(1)
M–S(5)	2.484(1)	2.644(1)	2.379(1)
M–S(14)	2.340(1)	2.480(1)	2.259(1)
M–S(17)	2.326(1)	2.875(1)	2.706(1)
N(24)–M–S(2)	85.10(8)	77.16(7)	82.09(10)
N(24)–M–S(14)	132.89(7)	125.36(7)	122.05(10)
N(24)–M–S(5)	115.96(7)	118.06(7)	122.00(10)
S(2)–M–S(5)	88.87(3)	82.73(3)	85.77(4)
S(2)–M–S(17)	169.66(3)	144.84(3)	157.94(4)
S(5)–M–S(14)	111.13(3)	111.38(3)	114.65(4)
S(5)–M–S(17)	95.62(3)	93.60(3)	92.43(4)

Ni–S(2) 84.52(7) and Cl(1)–Ni–S(17) 92.24(3)°]. The nickel atom is slightly displaced (0.23 Å) out of the equatorial NS_3Cl plane towards the axial Cl atom. Selected bond lengths and angles are summarized in Table 2.

Three five-membered and one ten-membered chelate rings are formed after complex formation. In this type of mixed donor system, ether and thio-ether donor atoms are expected to bind relatively more weakly to nickel than the nitrogen donors. As a consequence, any cumulative ring strain arising from the two five-membered fused rings (with pyridine nitrogen) might be expected to be relieved by changes in the bond lengths in the remaining five-membered chelate ring incorporating the sulfur donors. This results in one of the SCH_2CH_2S linkages adopting a *gauche* conformation accompanied by unequal Ni–S bond lengths [Ni–S(2) 2.380(1), Ni–S(17) 2.405(1) and Ni–S(5) 2.524(1) Å]. The equatorial Ni–Cl(1) bond [2.375(1) Å] is comparatively longer than the axial Ni–Cl(2) bond [2.362(1) Å] to maintain the square plane. The second SCH_2CH_2S linkage adopts an *anti* conformation resulting in a non-bonded S donor atom, S(14). A 14-membered macrocyclic ligand has a cavity which is usually too small for the nickel(II) ion to fit in,[12] whereas 15- and 16-membered ring macrocycles have a nearly ideal cavity size for the high-spin nickel(II) ion. Consequently one of the SCH_2CH_2S linkages in **12** has a folded configuration as described earlier (five-membered chelate ring) and another SCH_2CH_2S linkage is projected in such a way that one of the benzylic sulfur atoms is further away from the nickel(II) centre and remains uncoordinated.

The packing diagram for complex **12** along the *a*-axis shows that, in the solid state, two Ni·**11**·Cl_2 units are linked by hydrogen bonding between axial Cl(2) and the aromatic hydrogen of the *o*-xylyl group of the adjacent macrocycle and hence a ribbon like structure is obtained. The Ni–Cl ··· H–C-type of hydrogen bonding associated with this complex has a C ··· H distance of 2.842 Å and a Ni–Cl–H angle of 99.7°. The two adjacent ribbons are arranged in an anti-parallel fashion with a

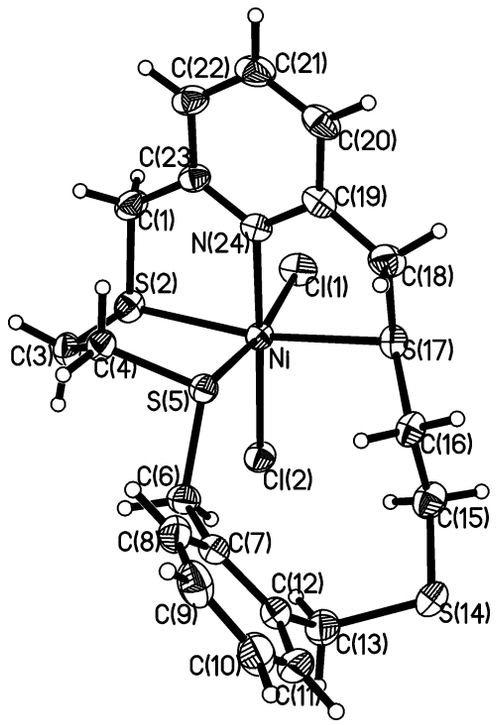

Fig. 2 ORTEP drawing of the Ni(II) complex **12**.

distance of 3.975 Å and there is no interaction between adjacent ribbons.

Structure description of complexes 13 and 14

X-Ray structural determination of the palladium complex **13** indicates that the macrocycle adopts a formal [4 + 1] coordination sphere (Fig. 3) at Pd(II). The N-donor of the pyridine

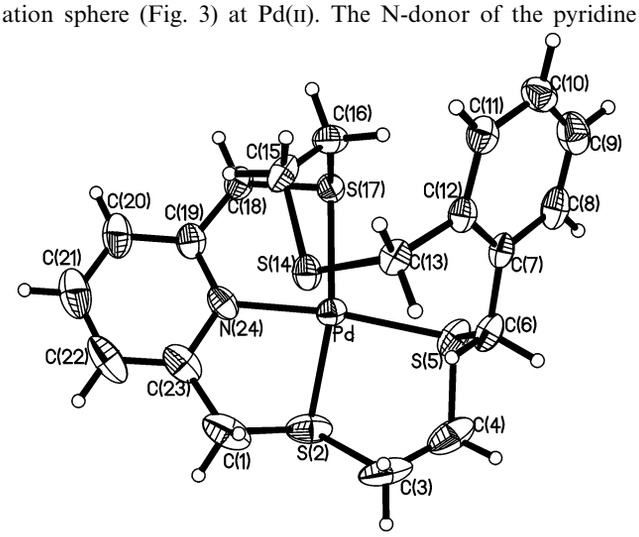

Fig. 3 ORTEP diagram of the cationic complex of **13**.

moiety [Pd–N 2.024(6) Å] and three of the four S-donors of the thio-ether linkages [Pd–S(2) 2.260(2), Pd–S(5) 2.312(2), Pd–S(17) 2.326(2) Å] constitute a slightly distorted square planar arrangement at the Pd(II) ion. The fourth S-donor [S(14)] occupies an apical site with a long range interaction to the metal centre [Pd ··· S(14) 3.036 Å] and the palladium is displaced 0.095 Å out of the NS_3 mean plane towards the apical sulfur atom [S(14)]. Related long range apical interactions to Pd(II) metal ion ranging from 2.9 to 3.2 Å have been reported previously in which a [4 + 2] or [4 + 1] coordination sphere is imposed by the macrocyclic ligands.[1–4,12]

The basal angles N(24)–Pd–S(5) and S(2)–Pdi–S(17) are 171.82(2) and 162.23(7)° respectively, which are in fair agreement with angles expected for a square pyramidal geometry around a d^8-metal ion. To form a square pyramidal geometry, the fourth sulfur atom occupies an apical site in which the SCH_2CH_2S linkage adopts a *gauche* conformation (torsion angles of about 60°). This leads to unequal metal–sulfur bond distances and angles in the complex (refer to Table 2).

The single crystal structure of the platinum complex [Pt·**11**]-$[PF_6]_2$ is iso-structural (Fig. 4) to [Pd·**11**][PF_6]$_2$. The main difference in the Pt(II) complex is a longer bond distance between the metal centre and the sulfur atom occupying the apical position of the square pyramid [Pt–S(14) 3.140 Å] and that the Pt(II) has a displacement of 0.068 Å out of the mean plane defined by the basal donor atoms towards the apical sulfur atom. A [4 + 2] or [4 + 1] coordination sphere is also common among macrocyclic Pt(II) complexes reflecting the preference of a square planar coordination by the d^8-metal ion.[12,26] Selected bond lengths and angles of both palladium and platinum complexes **13** and **14** are summarized in Table 2.

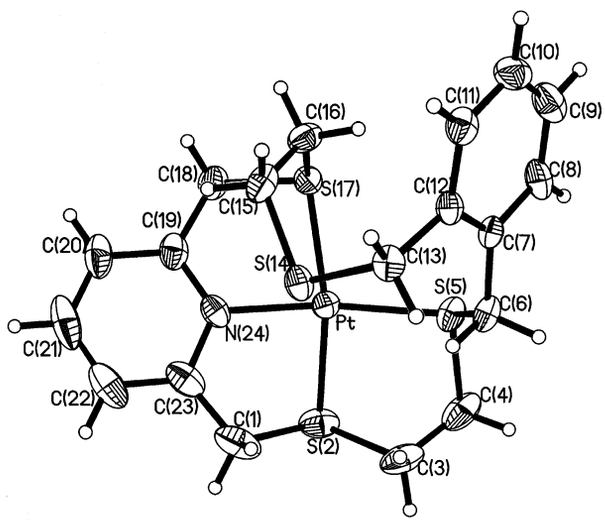

Fig. 4 ORTEP diagram of the cationic complex of **14**.

In the solid state, complexes **13** and **14** do not exist as discrete molecules but they are packed with some weak interactions. Both the complexes are crystallised with one water molecule. Three weak interactions of the type F ··· H–C are observed[27] (bond distances for **13**: 2.385, 2.403 and 2.521 Å; for **14**: 2.413, 2.494 and 2.521 Å). The existence of C–H ··· F hydrogen bonding is still being debated.[28] The resultant structure along the *b*-axis looks like a two-dimensional honeycomb while along the *c*-axis, a wave-like pattern is observed in both. The main difference between the complexes **13** and **14** is an additional weak interaction of the type H ··· S–C (2.935 Å) observed in the platinum complex and hence more extensive intermolecular interactions in the wave pattern of its crystal packing.

Structure description of complexes 15–17

Single crystals of the copper(II) complex **15** were obtained by ether diffusion of an acetonitrile solution of the complex. It is crystallised with one molecule of water. Using liquid diffusion of reactants, crystals suitable for X-ray diffraction studies were obtained for complex **16**. Quality crystals of the pale green complex of **17** were obtained by the slow solvent evaporation of its solution in a CH_2Cl_2–MeOH mixture. The crystal structures of **15**, **16** and **17** are shown in Figs. 5, 6 and 7 respectively. The molecular formulae for the above complexes are also confirmed by mass spectrometry and elemental analysis.

In all three complexes **15**–**17**, the central metal atom is coordinated to all five donor atoms of the macrocycle **11**. Bond angles and distances around the metal centre confirm that the metal centre adopts a coordination geometry that lies intermediate between a square pyramid or trigonal bipyramid. This

Table 3 Spectroscopic data for complexes **12**–**15** and **17**

Complex	Solvent	Solution colour	λ_{max}/nm (ε_{max}/dm^3 mol^{-1} cm^{-1})
Ni·**11**·Cl_2, **12**	DMSO	Green	240 (28320), 279 (21379), 308 (11598), 586 (41), 664 (39)
Pd·**11**·$(PF_6)_2$, **13**	CH_3CN	Red–orange	240 (28320), 290 (30570), 490 (154)
Pt·**11**·$(PF_6)_2$, **14**	CH_3CN	Light yellow	230 (23520), 264 (21269)
Cu·**11**·$(ClO_4)_2$, **15**	CH_3CN	Dark green	430 (3950), 598 (550)
Cu·**11**·PF_6, **17**	CH_3CN	Light green	426 (2334), 596 (304)

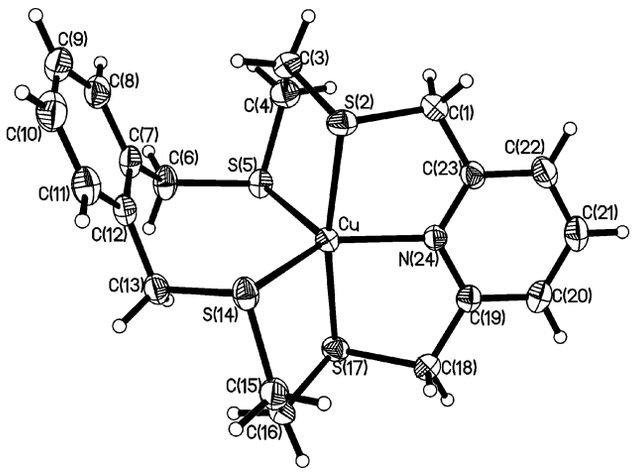

Fig. 5 ORTEP diagram of the cationic complex of **15**.

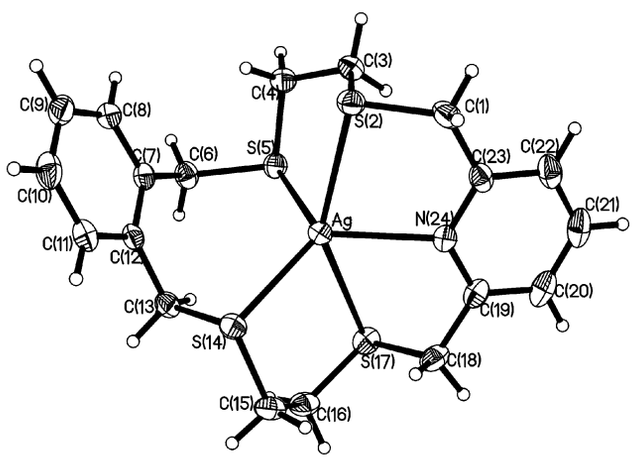

Fig. 6 ORTEP diagram of the cationic complex of **16**.

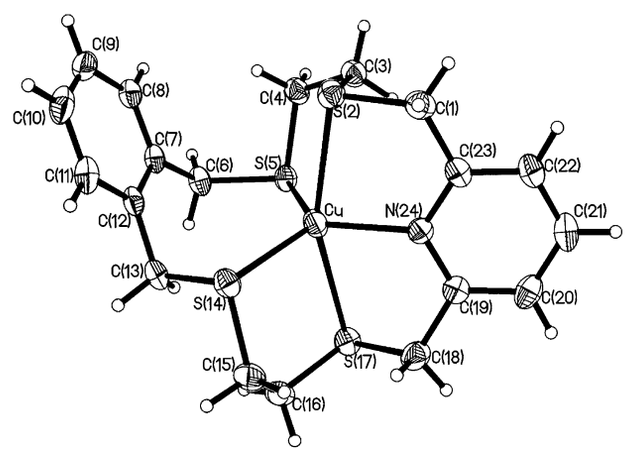

Fig. 7 ORTEP diagram of the cationic complex of **17**.

is further illustrated by a calculation of the degree of trigonality (τ) described by Addison *et al.*[29] The coordination geometry around copper in complexes **15** and **17** is thus better described as a square-based pyramidal distorted trigonal bipyramid (SBPDTB) and that for the silver complex **16** as a trigonal bipyramidal distorted square-based pyramid (TBDSBP).[30]

In both the copper complexes **15** and **17**, the pyridine nitrogen and two of the benzylic sulfur atoms form the trigonal plane [N(24), S(5) and S(14)] and the remaining two sulfur atoms [S(2) and S(17)] occupy the axial positions of the trigonal bipyramid. The Cu(II) and Cu(I) metal ions deviate by −0.015 and 0.148 Å respectively from the trigonal plane towards the axial S(2) donor atom. In Cu(II) the equatorial bond lengths are comparatively longer than the axial Cu–S bonds, but in the Cu(I) complex, the reverse is observed. This difference is mainly due to differences in the conformation of the SCH_2CH_2S linkages in the Cu(II) and Cu(I) complexes (see Figs. 5 and 7). Selected bond lengths and angles for complexes **15**–**17** are given in Table 2.

The mean equatorial Cu(II)–S bond distance of 2.412 Å and the Cu(II)–N distance of 2.005(2) Å in **15** are comparable with literature values.[31–34] Interestingly the mean equatorial Cu(I)–S distance of 2.319 Å is shorter while the Cu(I)–N distance of 2.103 Å is longer than the corresponding values in the copper(I) complex **17**. However, the Cu(I)–N distance is comparable with reported values for most Cu(I) complexes containing pyridine or substituted pyridine.[35]

The geometry around Ag(I) ion in complex **16** is better regarded as a very distorted trigonal bipyramid, which may be due to the larger metal ion and the size constraint in the macrocycle (Fig. 6). In its crystal structure, the trigonal plane is formed by the pyridine nitrogen [N(24)] and two of the benzylic sulfur atoms [S(5) and S(14)]; the other two sulfur atoms [S(2) and S(17)] occupy approximately axial positions. The S(2)–Ag–S(17) angle (144.84°) is considerably smaller than 180°. The Ag(I) ion is lies 0.33 Å above the equatorial plane, towards S(2). Like the Cu(I) complex **17**, the axial Ag–S bonds in **16** are comparatively longer than the equatorial bonds (see Table 2; Fig. 7). The Ag–N(24) and mean Ag–S bond lengths are comparable with reported values in the literature.[16]

In the crystal packing of complex **15**, dimers are found to be connected through weak S ··· S (3.467 Å) interaction and thereby resulting in linear chains but there is no interaction between the chains. The dimer is associated with three types of weak interactions: S ··· S (3.647 Å), two S ··· O (3.190 and 3.166 Å) and two C–H ··· O–Cl (2.456 and 2.561 Å). Unlike complex **15**, there is no interaction between the dimers in complex **17** because of the presence of PF_6^- anions between them. The dimer is associated with only two types of interactions: C–H ··· S (2.805 Å) and C–H ··· F (2.556 Å). A similar type of packing is observed in complex **16**. The only difference is that its dimers are connected through two PF_6^- molecules: one on each side and thereby a linear chain-like structure is obtained. There are four hydrogen bondings of the type C–H ··· F observed (2.441 and 2.498 Å) in between the dimers. The dimer experiences four interactions: two Ag ··· S (3.925 Å) and two Ag ··· H (3.331 Å) and there is a perfect square plane observed in this dimer [S(14A), Ag(1), Ag(2) and S(14B)].

UV-Visible spectroscopic study of complexes 12–15 and 17

The details of the electronic absorption of the complexes is given in Table 3. The absorption peaks for palladium complex **13** are observed at 290 and 490 nm. The higher energy band is

attributed to the intense π–π* transitions and the less intense lower energy band can be assigned to a CT transition. Similar transitions appeared at 230 and 264 nm in the platinum complex **14**. Both the transitions are considered as intra-ligand transitions as they fall below 400 nm. The copper(II) complex **15** is intensely coloured with strong absorption bands at 430 and 598 nm, the former being relatively more intense. These two bands are attributed to S(σ) ⟶ Cu(II) and S(π) ⟶ Cu(II) charge-transfers, respectively. These bands are of considerable interest as the intense visible absorptions exhibited by the blue copper proteins are attributed to similar S ⟶ Cu charge-transfers, although a coordinated mercaptide sulfur (cysteine) is involved in the latter case.[36]

Redox properties of complexes 13, 14, 15 and 17

The redox properties of $[M\cdot\mathbf{11}]^{2+}[PF_6]^-_2$ (M = Pd and Pt) **13** and **14** were monitored by cyclic voltammetry using acetonitrile as a solvent and tetraethylammonium tetrafluoroborate was used as a supporting electrolyte. The potential window was selected in the range of +0.3 to −2.0 V *vs*. Ag/AgCl. At this potential the macrocycle **11** and the supporting electrolyte were found to be inert. In the cyclic voltammograms of the Pd(II) and Pt(II) complexes, only one irreversible reduction peak was observed in each case. The peak shifted to a more negative potential with increasing scan rate. The broad irreversible reduction peaks appeared at −0.994 and −1.368 V for **13** and **14** respectively. The above results suggest that the reduction of the Pd(II) and Pt(II) complexes occurs at relatively accessible potentials. The Pd(I) and Pt(I) radical species generated were transient and quenched rapidly. Attempts are in progress in our laboratory to stabilize the Pd(I) and Pt(I) complexes by modifying the structural and donor nature of the macrocyclic ligands.

The cyclic voltammograms of $[Cu\cdot\mathbf{11}]^{2+}[ClO_4]^-_2$ **15** and $[Cu\cdot\mathbf{11}]^{2+}[PF_6]^-$ **17** are shown in Fig. 8. For **15** it was found that $E_{1/2}$

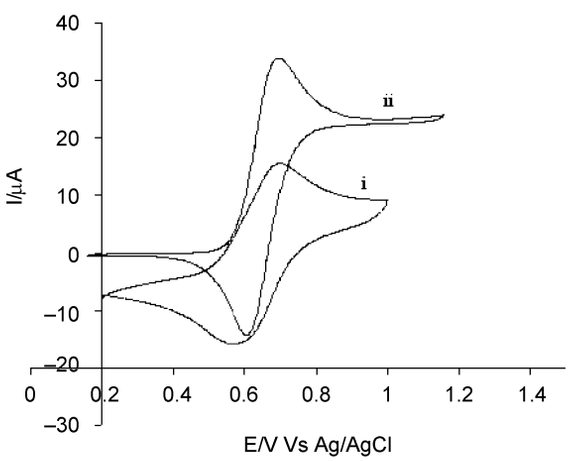

Fig. 8 The cyclic voltammogram of (i) complex **15** and (ii) complex **17**.

occurs at 0.7 V *vs*. Ag/AgCl, and the cathodic reduction peak occurs at 0.57 V. The $Cu^{I/II}$ couple appears to be a reversible system with well-defined anodic and cathodic peaks. The $E_{1/2}$ value of **17** is essentially identical to that of **15** at 0.7 V while the cathodic reduction peak occurs at 0.6 V. The ΔE value is slightly decreased (0.1 V) which indicates that the electron transfer process involves lower energy thus implying a less stable compound. This is consistent with a shift in the cathodic reduction potential to a less positive value going from **17** to **15** indicating a relatively more stable compound. The $E_{1/2}$ values of the complexes **13**–**15** and **17** are comparable to values reported in the literature.[16] The relatively poor solubility of the nickel complex **12** in most organic solvents prevented a study of its redox chemistry.

Metal ion extraction study

The complexing ability of the macrocycle **11** to selected transition metal cations Ag(I), Cd(II), Cu(II), Co(II), Hg(II), Ni(II), Pb(II) and Zn(II) was assessed by solvent extraction of the metal chlorides from aqueous solutions into chloroform. The procedure employed was similar to those reported by Kumar *et al.* and Nishimura *et al.* in their investigation of cyclophanes with mixed nitrogen and sulfur/oxygen donors.[37,38] The results from our work are summarized in Fig. 9. The overall observation was that **11** does not show any significant selectivity among the series of metal ions but it extracts all these metal ions appreciably. An approximate extraction selectivity order is Cu(II), Ni(II), Co(II), Pb(II) > Cd(II), Hg(II) > Ag(I) > Zn(II). Thus, **11** exhibits a relatively low preference for Zn(II).

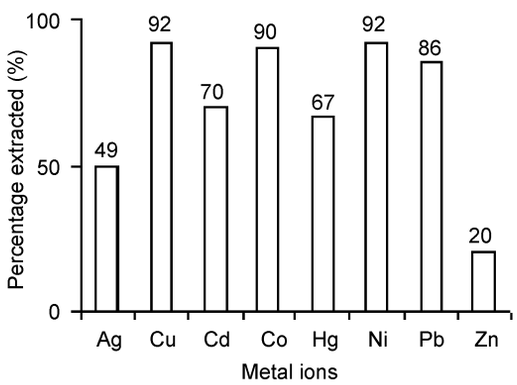

Fig. 9 Relative extraction profile of the macrocycle **11**.

Conclusion

A new pentadentate macrocyclic ligand [17]aneNS$_4$ **11** containing mixed donor atoms has been synthesized by using a high-dilution procedure and characterized by spectroscopic and X-ray crystallographic studies. Its Ni(II), Pd(II), Pt(II), Cu(II), Ag(I) and Cu(I) complexes **12**–**17** were prepared and their crystal structures were investigated by using X-ray crystallography. The macrocycle **11** serves as a tetradentate ligand in the Ni(II) complex **12**; it behaves like a tetradentate ligand in the Pd(II) and Pt(II) complexes **13** and **14** but there is a weak interaction between the fifth sulfur atom in **11** with the metal ion. In the Cu(II), Ag(I) and Cu(I) complexes **15**–**17** the macrocycle **11** truly acts as a pentadentate ligand. The above observation illustrates the flexibility of the macrocycle **11** in adopting different structural conformations and coordinating behaviour to bind to the various metal ions effectively. The extraction property of the macrocycle **11** shows poor selectivity among a series of metal ions but it exhibits a significantly lower preference for the Zn(II) ion.

Acknowledgements

This work was supported (R-143-000-026-112) by the National University of Singapore (NUS), Singapore. M. V. thanks the NUS for a research scholarship. Assistance from the technical staff of the Department of Chemistry, NUS, is gratefully acknowledged.

References

1 M. P. Suh, K. Y. Oh, J. W. Lee and Y. Y. Boe, *J. Am. Chem. Soc.*, 1996, **118**, 777.
2 A. McAuley, P. R. Norman and O. Olubuyide, *Inorg. Chem.*, 1984, **23**, 1938.
3 L. Fabrizzi, T. A. Kaden, A. Perotti, B. Seghi and L. Siegfried, *Inorg. Chem.*, 1986, **25**, 321.
4 A. J. Blake, R. D. Crofts, B. De Groot and M. Schröder, *J. Chem. Soc., Dalton Trans.*, 1993, 2259 and refs. therein.

5 J. D. Woollins and P. F. Kelly, *Coord. Chem. Rev.*, 1985, **65**, 115.
6 A. McAuley and T. W. Whitecombe, *Inorg. Chem.*, 1988, **27**, 3090.
7 G. J. Grant, K. A. Sounders, W. N. Setzer and D. G. Van Derveer, *Inorg. Chem.*, 1991, **30**, 4053.
8 A. J. Blake, G. Reid and M. Schröder, *J. Chem. Soc., Dalton Trans.*, 1990, 3363 and refs. therein.
9 S. R. Cooper, *J. Am. Chem. Soc.*, 1991, **113**, 1660.
10 A. J. Blake, R. O. Gould, J. A. Grieg, A. J. Holder, T. I. Hyde, A. Taylor and M. Schröder, *Angew. Chem., Int. Ed. Engl.*, 1990, **29**, 197.
11 K. R. Adam, D. S. Baldwin, P. A. Duckworth, L. F. Lindoy, M. McPartlin, A. Bashall, H. R. Powell and P. A. Tasker, *J. Chem. Soc., Dalton Trans.*, 1995, 1127.
12 F. Contu, F. Demartin, F. A. Devillanova, A. Garau, F. Isaia, V. Lippolis, A. Salis and G. Verani, *J. Chem. Soc., Dalton Trans.*, 1997, 4401 and refs. therein.
13 M. G. B. Drew, C. Cairns, S. M. Nelson and J. Nelson, *J. Chem. Soc., Dalton Trans.*, 1981, 942 and refs. therein.
14 A. W. Addison, T. Nageswara and E. Sinn, *Inorg. Chem.*, 1984, **23**, 1957.
15 L. F. Lindoy and D. H. Busch, *Inorg. Chem.*, 1974, **13**, 2494.
16 G. Reid and M. Schröder, *Chem. Soc. Rev.*, 1990, **19**, 239.
17 S. J. Loeb and K. D. L. Smith, *Inorg. Chem.*, 1993, **32**, 1297.
18 E. C. Constable, A. C. King and P. R. Raithby, *Polyhedron.*, 1998, **17**, 4275.
19 G. M. Sheldrick, SHELXL 93, Program for Crystal Structure Refinement, University of Göttingen, 1993.
20 L. A. Drummond, K. Henrick, M. J. L. Kanagasundaram, L. F. Lindoy, M. McPartlin and P. A. Tasker, *Inorg. Chem.*, 1982, **21**, 3923 and refs. therein.
21 S. J. Loeb and G. K. H. Shimizu, *Synlett.*, 1992, 823.
22 J. J. H. Edema, J. Buter, R. M. Kellog, A. L. Spek and F. Van Balhuis, *J. Chem. Soc., Chem. Commun.*, 1992, 1558 and refs. therein.
23 K. R. Adam, L. G. Brigden, K. Henrick, L. F. Lindoy, M. McPartlin, B. Mimnagh and P. A. Tasker, *J. Chem. Soc., Chem. Commun.*, 1985, 710.
24 D. G. Fortier and A. McAuley, *Inorg. Chem.*, 1989, **28**, 655.
25 U. Kallert and R. Mattes, *Inorg. Chim. Acta*, 1991, **180**, 263 and refs. therein.
26 F. Contu, F. Demartin, F. A. Devillanova, A. Garau, F. Isaia, V. Lippolis, A. Salis and G. Verani, *J. Chem. Soc., Dalton Trans.*, 1997, 4401 and refs. therein.
27 P. A. Duckworth, F. S. Stephens, K. P. Wainwright, K. D. V. Veerasuria and S. B. N. Wild, *Inorg. Chem.*, 1989, **28**, 4531.
28 D. Barga, F. Grepioni and G. R. Desiraju, *Chem. Rev.*, 1998, **98**, 1375.
29 A. W. Addison, T. N. Rao, J. Reedijk, J. Van Rijn and G. C. Verschoor, *J. Chem. Soc., Dalton Trans.*, 1984, 1349.
30 G. Murphy, C. O'Sullivan, B. Murphy and B. Hathaway, *Inorg. Chem.*, 1998, **37**, 240.
31 B. J. Hathaway, *Coord. Chem. Rev.*, 1983, **52**, 87.
32 W. N. Setzer, C. A. Ogle, G. S. Wilson and R. S. Glass, *Inorg. Chem.*, 1983, **22**, 266.
33 L. Escriche, M. Sanz, J. Casabo, F. Teixidor, E. Molins and L. Miravitlles, *J. Chem. Soc., Dalton Trans.*, 1989, 1739.
34 N. Atkinson, A. J. Blake, M. G. B. Drew, G. Forsyth, R. O. Gould, A. J. Lavery, G. Reid and M. Schröder, *J. Chem. Soc., Dalton Trans.*, 1992, 2993.
35 F. R. Fronczek, P. J. Schilling, S. F. Watkins, V. K. Majestic and G. R. Newcomb, *Inorg. Chim. Acta*, 1996, **246**, 119 and refs. therein.
36 D. B. Rorabacher, M. J. Martin, M. J. Koenigbauer, M. Malik, R. R. Schroeder and J. F. Endicott in *Copper Coordination Chemistry; Biochemical and inorganic Perspectives*, eds. K. D. Karlin and J. Zubieta, Adenine press, New York, 1983.
37 S. Kumar, M. S. Hundal, G. Hundal, P. Singh, V. Bhalla and H. Singh, *J. Chem. Soc., Perkin Tran.s 2*, 1998, 925.
38 S. Inokuma, K. Kimura, T. Funaki and J. Nishimura, *Heterocycles.*, 2001, **54**, 123.
39 M. N. Burnett and C. K. Johnson, ORTEP-III: Oak Ridge Thermal Ellipsoid Plot Program for Crystal Structure Illustrations, Report ORNL-6895, Oak Ridge National Laboratory, Oak Ridge, TN, USA, 1996.